HHS Public Access

Author manuscript

Nat Med. Author manuscript; available in PMC 2013 October 01.

Published in final edited form as:

Nat Med. 2013 April ; 19(4): 458–464. doi:10.1038/nm.3108.

Differential innate immune response programs in neuronal subtypes determine susceptibility to infection in the brain by positive stranded RNA viruses

Hyelim Cho[1], **Sean C. Proll**[4], **Kristy J. Szretter**[2], **Michael G. Katze**[4], **Michael Gale Jr.**[5], and **Michael S. Diamond**[1,2,3]

[1]Department of Molecular Microbiology, Washington University School of Medicine, St. Louis, Missouri 63110

[2]Department of Medicine, Washington University School of Medicine, St. Louis, Missouri 63110

[3]Department of Pathology and Immunology, Washington University School of Medicine, St. Louis, Missouri 63110

[4]Department of Microbiology, University of Washington School of Medicine, Seattle, WA 98195-7650

[5]Department of Immunology, University of Washington School of Medicine, Seattle, WA 98195-7650

Abstract

Although susceptibility of neurons in the brain to microbial infection is a major determinant of clinical outcome, little is known about the molecular factors governing this. Here, we show that two types of neurons from distinct brain regions exhibited differential permissivity to replication of several positive-stranded RNA viruses. Granule cell neurons (GCN) of the cerebellum and cortical neurons (CN) from the cerebral cortex have unique innate immune programs that confer differential susceptibility to viral infection *ex vivo* and *in vivo*. By transducing CN with genes that were expressed more highly in GCN, we identified three interferon-stimulated genes (ISGs; *Ifi27*, *Irg1*, and *Rsad2/Viperin*) that mediated antiviral effects against different neurotropic viruses. Moreover, we found that the epigenetic state and microRNA-mediated regulation of ISGs correlates with enhanced antiviral response in GCN. Thus, neurons from evolutionarily distinct brain regions have unique innate immune signatures, which likely contribute to their relative permissiveness to infection.

Corresponding author: Michael S. Diamond, M.D., Ph.D., Departments of Medicine, Molecular Microbiology and Pathology & Immunology, Washington University School of Medicine, 660 South Euclid Avenue, Box 8051, St Louis. Missouri 63110. Tel: 314-362-2842. Fax: 314-362-9230. diamond@borcim.wustl.edu.

AUTHOR CONTRIBUTIONS

H.C and K.J.S. performed the experiments. H.C. and S.C.P. analyzed the microarray data. H.C. and M.S.D. designed the experiments and wrote the initial draft of the manuscript. M.G.K. and M.G. contributed to the study design and preparation of the manuscript.

COMPETING FINANCIAL INTERESTS

The authors have no financial conflicts to disclose.

Virus infection of mammalian cells induces signaling pathways that promote an antiviral state. RNA intermediates of virus replication are recognized by pathogen recognition receptors (PRR), such as Toll-like receptors (TLR) and RIG-I-like receptors (RLR), which signal specific transcription factors to induce innate defense programs, including type I interferon (IFN) expression and secretion. Binding of IFN to IFN-αβ receptor (Ifnar) on infected and uninfected cells results in a signaling cascade that restricts infection of many viruses through expression of interferon-stimulated genes (ISGs). Several studies report that type I IFN receptor-knockout mice (*Ifnar*$^{-/-}$) exhibit enhanced mortality after viral infection due to increased viral burden and expanded tropism in neurons of the brain[1,2].

Neurotropic viruses use many strategies to enter the central nervous system (CNS) and spread between different subtypes of neurons to establish acute or persistent infection[3]. Neurons are not passive targets, as they participate in the host immune response against viruses by producing and responding to type I IFN[4] through Stat1-dependent signaling pathways[5–7]. Autopsy studies have reported differential susceptibility of neurons to West Nile virus (WNV) in the human brain with sparing of infection in granule cell neurons of the cerebellum compared to adjacent Purkinje neurons or neurons in the cerebral cortex[8]. Analogous to this, herpes simplex virus localizes primarily to the temporal lobes of the cerebral cortex and causes encephalitis and cognitive impairment[9].

A comprehensive understanding of innate immune programs against viral infection in specific neurons, and how this relates to regional susceptibility in the CNS, remains unexplored. Moreover, the function of specific antiviral ISGs in neuronal subtypes also has not been established. Here, we defined innate immune gene programs in response to viral infection or IFN-β treatment of two developmentally disparate populations of neurons with differential susceptibility to replication of WNV and other positive strand RNA viruses. We show that specific neurons of the cerebellum and cerebral cortex have unique host defense signatures including expression of key novel antiviral genes, which confer differential permissiveness to infection by multiple neurotropic viruses.

RESULTS

Cerebellar granule cell neurons are more sensitive to the antiviral effects of IFN-β than cortical neurons

Type I IFN restricts WNV infection in the brain[10,11] in part, by limiting viral replication in neurons. Granule cell neurons (GCN) of the cerebellum and cortical neurons (CN) from the cerebral cortex are differentially permissive for WNV infection in humans[8,12]. To determine whether these neurons respond uniquely to antiviral cytokines and infectious challenge, we infected GCN and CN cultures with WNV in the presence or absence of IFN-β treatment. While IFN-β pre-treatment (100 IU/ml, 24 hours) inhibited WNV replication in CN by 15-fold ($P < 0.0001$), it reduced infection ~100 fold ($P < 0.0001$) in GCN at 24 to 48 hours after infection (Fig 1a). A greater responsiveness to IFN-β in GCN compared to CN also was observed with other positive-stranded RNA viruses including a flavivirus (Saint Louis encephalitis virus (SLEV), up to 95-fold), an alphavirus (Venezuelan equine encephalitis virus (VEEV), up to 10,000-fold, $P < 0.0001$), and a coronavirus (mouse hepatitis virus (MHV), up to 200-fold, $P < 0.0005$) (Fig 1b–d). GCN also were less permissive for WNV

replication at baseline in the absence of IFN-β treatment (15 to 110-fold lower titers at 24 and 48 hours, $P < 0.0001$) (Fig 1a), with similar findings observed with SLEV (up to 700-fold, $P < 0.005$), VEEV (up to 200-fold, $P < 0.05$), and MHV (up to 20-fold, at 24 and 36 hours, $P < 0.0001$) (Fig 1b–d). The percentage of cells infected by WNV was greater in CN compared to GCN at baseline or after IFN-β pre-treatment (Supplementary Fig 1). Consistent with the observation of greater infection of CN, the concentration of type I IFN secreted into the supernatant after WNV infection was higher in CN compared to GCN cultures (Supplementary Fig 2).

Antiviral genes and host defense pathways are differentially regulated in two neuronal subtypes

We performed microarray and pathway analysis to model molecular networks and define whether distinct antiviral IFN responses occurred in the two subtypes of neurons. Global gene expression in GCN and CN in response to IFN-β treatment revealed overlapping yet distinct gene signatures (Fig 2a). Computational analysis revealed that genes associated with type I IFN induction (PRR (e.g., TLR and RLR)) and IFN regulatory factors (e.g., *Irf1*, *Irf7*, and *Irf*9) and effector function (e.g., *Mx1* and *Oas*) were induced in both GCN and CN (Supplementary Table 1). We speculated that the two neuronal subtypes might differentially express key host defense genes at the basal level, which could impact responsiveness to IFN and susceptibility to infection. Indeed, the basal and IFN-β-induced levels of genes involved in IFN induction, signaling, and effector function generally were higher in GCN (Fig 2b, $P < 0.01$), and included *Irf7*, *Stat1*, *Ifit1*, and *Oas1* (Supplementary Table 2). This pattern, which was confirmed by qRT-PCR (Supplementary Fig 3), suggests that the greater IFN sensitivity of GCN may be due to higher basal expression of PRR and IFN signaling genes. Indeed, some of the ISGs (e.g., *Stat1*, *Ifi27*, and *Rsad2)* showed differential basal expression yet similarly induced levels of expression after IFN-β treatment. Other ISGs (e.g., *Ccl5* and *Cxcl5*) showed differences in expression patterns between IFN-β treated and WNV-infected cells. This may reflect variation in IFN-dependent and IFN-independent gene induction that occurs in the context of WNV replication and recognition by intracellular PRRs.

To identify nodes of gene regulatory network interaction that corresponded to specific antiviral or immune pathways, we performed computational analysis on genes with statistically significant expression changes. We detected an enrichment of genes with functions associated with immune responses to viral infection. Canonical PRR signaling through TLR and RLR pathways (e.g., *Tlr7*, *Ddx58/Rig-I*, and *Ifih1/Mda5*), transcription factors (e.g., *Nfκ**B*, *Irf7*, and *Irf*9), and their corresponding target genes (e.g., *Ccl5* and *Tnf-α*) were expressed at higher levels in GCN at the basal level (Supplementary Table 2). In particular, *Stat1* and IFN signaling-dependent genes (e.g., *Ifit1*, *Ifit3*, *Oas*, and *Mx1*) also were expressed in GCN basally at higher levels compared to CN. In resting or IFN-β-treated GCN, we observed an enrichment of genes that have been linked to antiviral activity (e.g., *Ifit1*, *Rsad2*, *Oas1*, *Irf7*, *Bst2/Tetherin*, *Unc93b1*, *Ifih1/Mda5*, *Ddx58/Rig-I*, *Mx1*, *Ikbkε/Ikkε*, and *Stat1*), autophagy and inflammation (immune-related GTPases (*Irgm1*, *Irgm2*, *Igtp/Irgm3*, and *Ifi47/Irg47*, *Tgtp1/Irgb6*)), and leukocyte chemotaxis (*Ccl5*, *Cxcl1*, *Cxcl10*, and *Cxcl16*) (Supplementary Fig 4 and Supplementary Table 2). This pattern of gene expression

is consistent with results showing that GCN are less permissive to virus replication at baseline or in the presence of IFN-β treatment (Fig 1a–d).

Some antiviral ISGs (e.g., *Ifit1*, *Rsad2*, and *Oas*) reached peak expression levels sooner in GCN compared to CN after IFN-β treatment (Fig 3). Thus, a higher basal expression of host defense genes makes GCN more poised than CN for antiviral action in response to IFN-β, and ultimately impacts the induced level expression of ISGs. Notably, addition of a blocking monoclonal antibody to Ifnar restored (~20-fold, $P < 0.0001$) WNV replication in GCN, yet had little effect in CN (Fig 1f). Thus, the lower susceptibility of GCN to viral replication compared to CN at baseline is not likely attributed to differences in virus entry, but rather to higher expression of genes with an IFN signature, which confer greater responsiveness to the antiviral effects of type I IFN.

In contrast to virulent lineage 1 WNV strains (e.g., WNV-New York 1999 (WNV-NY)), a lineage 2 strain (WNV-Madagascar 1978 (WNV-MAD)) is impaired in its ability to antagonize phosphorylation of Stat1 and resultant IFN signaling, and thus, is more sensitive to its antiviral actions[13,14]. We hypotheiszed that IFN-β would have a greater antiviral effect on WNV-MAD in CN compared to WNV-NY. Indeed, WNV-MAD infection was restricted to a greater degree (~300 fold for WNV-MAD at 24 hours after infection, $P < 0.0001$) after IFN-β treatment of CN (Fig 1e). In comparison, the inhibitory effect of IFN-β against WNV-MAD and WNV-NY was more equivalent (~80-fold compared to ~50 fold at 24 hours after infection, $P < 0.0001$) in GCN. These results support the idea that Stat1-dependent signaling proteins are expressed at greater levels basally in GCN (Supplementary Fig 5) and contribute to the enhanced responsiveness to the antiviral activity of IFN-β in this cell type. To establish whether differential expression of ISGs was due to Stat1-dependent signaling, studies were repeated in *Stat1*$^{-/-}$ and wild-type GCN. *Stat1*$^{-/-}$ GCN showed lower basal expression of several ISGs compared to wild-type GCN (Supplementary Fig 6).

Identification of novel antiviral ISGs in primary neurons

Because of the enhanced responsiveness to the antiviral actions of IFN-β in GCN, we hypothesized that at least a subset of differentially expressed ISGs would confer inhibitory effects against WNV. We attempted to create a GCN-like antiviral phenotype in CN by ectopically expressing individual GCN-specific genes in CN. Candidate genes included ones showing higher expression at the basal level (e.g., *Irg1*, *Ifi27*, *Ifi44*, *Isg15*, *Bst2/tetherin*, *Rsad2*, *Ifitm3*, *Ifi204*, *Trim30*, *and Casp12*) or greater induction after IFN-β treatment (e.g., *Ifit2*, *Cmpk2*, and *Lcn2*) in GCN (Supplementary Table 2). *Irf1*, which was reported as a broad-acting antiviral signaling molecule[15,16], was included as a positive control. We developed a high-efficiency (~90%) lentivirus transduction system for ectopic expression of ISGs in primary neurons (Fig 4a). Thirty-nine ISGs were cloned, transduced into CN, and their antiviral effects were assessed in the absence or presence of exogenous IFN-β (Fig 4, and data not shown). Three genes (*Irg1*, *Ifi27*, and *Rsad2*) resulted in reduced (5 to 20-fold, $P < 0.05$) WNV yield when expressed ectopically in CN (Fig 4b and c); analogously, reduced viral infection with expression of these genes also was observed with SLEV (3 to 10-fold, $P < 0.0001$) and WNV-MAD (5 to 20-fold, $P < 0.0001$) (Fig 4f and g). Ectopic expression of *Irg1* (7-fold $P < 0.0005$) and *Ifi27* (3-fold $P < 0.01$) but not *Rsad2* ($P > 0.05$)

inhibited MHV infection (Fig 4h). Ectopic expression of these three genes (or any of the other ISGs tested) did not alter cell viability (Fig 4d, and data not shown) or confer an antiviral effect when tested in parallel against VEEV (Fig 4e); thus it is unlikely that the antiviral effect observed with WNV was due to cellular stress. Moreover, transduction of shRNA against *Ifi27*, *Irg1*, or *Rsad2* in GCN correspondingly resulted in enhanced infection of WNV-MAD (~10-fold, $P < 0.0001$) (Fig 4i).

Epigenetic and microRNA-mediated regulation of ISG expression in CN

As a recent study showed that cell type-specific differences in ISG expression can be attributed in part to epigenetic mechanisms[17], and because histone acetylation of ISGs has been implicated in the regulation of an antiviral state[18–20], we hypothesized that our innate immune phenotypes in GCN and CN might be associated with distinct patterns of histone modification. To investigate this, CN were pre-treated with the histone deacetylase (HDAC) inhibitor trichostatin A (TSA), infected with WNV, and virus infection was evaluated. While treatment with the HDAC inhibitor did not alter cell viability under the conditions tested (Fig 5a, *right*), it reduced viral yields (5-fold, $P < 0.0001$) (Fig 5a, *left*) and resulted in de-repression of expression of ISGs that had otherwise exhibited low basal expression levels in CN (Fig 5b).

Stat1 requires its co-activator p300/CBP, a histone acetyltransferase to enhance ISG transcription[21–23]. Our inhibitor experiments suggested that differential histone acetylation contributes to the lower basal expression of Stat1 and key ISGs in CN. One candidate for regulating this is microRNA-132, which is required for morphogenesis of cortical and hippocampal neurons, targets p300, and negatively regulates IFN-β and IL-1β signaling and antiviral immunity[24–26]. Expression of microRNA-132 reportedly is higher in the cerebral cortex compared to the cerebellum of rats and humans[27,28]. We also observed higher expression of microRNA-132 in CN and the cerebral cortex compared to GCN and the cerebellum (Fig 5c). Moreover, ectopic expression of microRNA-132 in GCN (Fig 5d) decreased expression of some ISGs (Fig 5e) but did not change expression of non-ISGs (Fig 5f). However, no change in viral yield was detected when microRNA-132 was expressed ectopically in GCN (data not shown). We suggest that the distinct antiviral programs observed between GCN and CN are explained in part by differences in the epigenetic state of key genes, which is influenced by the expression of specific microRNA.

Differential expression of ISGs in the cerebellum and cerebral cortex of naïve mice

Our results with primary neurons suggested that basal expression of host antiviral genes in GCN resulted in lower permissiveness to virus replication. To establish this *in vivo*, we used fluorescence *in situ* RNA hybridization. Brain tissues from naïve mice were hybridized with labeled probes to visualize relative levels of key antiviral genes (e.g., *Irg1* and *Ifi27*) and *Stat1* that showed differential basal expression *ex vivo* in GCN and CN (see Supplementary Table 2). While basal expression of a housekeeping gene was equivalent, expression of *Irg1*, *Ifi27*, and *Stat1* mRNA appeared qualitatively in greater abundance in neurons of the granule cell layer of the cerebellum compared those in the cerebral cortex (Supplementary Fig 7a–d). These results were validated quantitatively using a branched DNA amplification assay (Fig 6a).

GCN are less susceptible than CN to WNV replication in wild type but not *Ifnar*$^{-/-}$ mice

To validate our findings *in vivo*, we performed immunohistochemistry for detection of WNV antigen in the brains of wild type mice that were infected via an intracranial (i.c.) route. GCN of the contralateral cerebellum were less vulnerable to WNV infection compared to CN of the contralateral cerebral cortex (Fig 6b, *top panels* and Fig 6c), with less infection observed in neurons of the granule cell layer, even six days after infection. While our primary culture data suggests this phenotype is due to an inherent resistance of GCN because of a basal and rapidly activated antiviral program, it also is possible that productive infection of GCN occurs *in vivo* during the first few days but is cleared more rapidly. The low level of GCN infection, however, was not due to inefficient viral spread to the cerebellum, since the adjacent Purkinje cell neurons were infected. In comparison, in the brains of *Ifnar*$^{-/-}$ mice, comparable levels of WNV antigen were detected in both CN and GCN after i.c. infection (Fig 6b, *bottom panels*). Quantitation of infectious WNV from the cerebellum and the cerebral cortex of wild type and *Ifnar*$^{-/-}$ mice supported these results (Supplementary Fig 8).

GCN are less susceptible than CN to WNV replication in humans that succumb to fatal encephalitis

To corroborate these observations, we performed immunohistochemistry to detect viral antigen in the brains from seven human patients who succumbed to fatal WNV encephalitis. Analogous to our findings in mouse neurons, GCN were relatively spared from WNV replication compared to other neuronal populations (e.g., adjacent Purkinje neurons in the cerebellum and cortical neurons in the cerebral cortex) (Fig 6d, Supplementary Fig 9, and data not shown).

DISCUSSION

Comparison of neuronal cell types from functionally and evolutionarily distinct regions of the brain allowed us to identify gene signatures that correspond to unique antiviral signaling pathways. Our data revealed that genes associated with host defense pathway are more highly expressed in GCN at both the basal level and after IFN-β treatment. This included a Stat1 and IFN-dependent signaling signature that was expressed in uninfected GCN at higher levels compared to CN, which resulted in reduced permissiveness to replication of several neurotropic viruses.

GCN comprise the largest population of neurons in the brain and account for greater than 90% of neurons in the cerebellum alone[29]. Neuronal injury associated with extensive infection of GCN might cause defects in motor movement and learning, posture, and balance[30]. In additional to our identification of distinct host defense signatures of specific neuronal subtypes, cell-extrinsic effects of resident glial cells also could contribute to innate immune programming of neurons. A recent study demonstrated regional differences in basal chemokine and cytokine secretion by astrocytes grown from the cerebral cortex, cerebellum, and spinal cord[31], although no differences in type I IFN production were reported. While it is possible that glial cells contribute to the neuron-specific infection pattern observed *in vivo*, our primary neuron cultures lack astrocyte contamination and thus cell-extrinsic

regulation cannot explain the differential infectivity and innate gene expression patterns of GCN and CN observed in culture.

Characterization of the distinct antiviral programs in the two neuronal subtypes enabled us to identify antiviral genes against WNV and some (SLEV and MHV) but not other (VEEV) positive-stranded RNA viruses, including *Ifi27, Irg1,* and *Rsad2,* all of which exhibited higher basal and IFN-β-induced expression in GCN compared to CN. *Ifi27* was first suggested to have antiviral activity against Sindbis virus infection in mice[32] and also may attenuate infection of hepatitis C virus[33], although its mechanism of action remains unknown. *Irg1* is induced in macrophages and tissues from mice infected with the intracellular parasite, *Toxoplasma gondii* or bacteria, *Listeria monocytogenes*[34]. To date, no antimicrobial functions have been ascribed to this gene although it associates with the mitochondria, a site of regulation for PRR adaptor molecules and the antiviral signalosome[34,35]. Ectopic expression of *Rsad2* in CN also showed an antiviral effect against WNV infection, results that are consistent with recent studies in *Rsad2*$^{-/-}$ mice[36]. *Rsad2* is an endoplasmic reticulum (ER)-associated protein that has reported antiviral activity against several viruses, possibly because it inhibits bulk protein secretion, lipid raft formation, and virus budding, and localizes to ER-derived lipid droplets[37].

Our pathway analysis identified a unique IFN-β-inducible host defense signature; immune-related GTPases (IRGs). IRGs (*Irgm1*, *Irgm2*, *Igtp/Irgm3*, *Ifi47/Irg47,* and *Tgtp1/Itgb6*) are associated with autophagy and resistance to *Toxoplasma gondii*[38,39] and were expressed preferentially at the basal level in GCN. This may be relevant as *Toxoplasma gondii* infection in the CNS results in lesions of the frontal and parietal cortex, with sparing of the cerebellum[40,41]. While further study is warranted, the distinct basal expression of immunity-related GTPases or other host defense proteins may contribute to regional susceptibility of the brain of *Toxoplasma gondii*[42], and explain more generally neuronal subtype-specific differences to microbial pathogenesis.

Why do GCN of the cerebellum express a higher basal level of host defense genes than CN? We observed a large number of Stat1-dependent genes that were expressed at higher levels in the basal and induced states in GCN compared to CN. Unphosphorylated Stat1 can promote expression of antiviral genes without IFN-dependent stimulation[43], and higher basal levels of Stat1 can amplify cell-intrinsic immune responses by activating an amplification loop[44,45]. Stat1 and its downstream gene targets could be differentially regulated in GCN and CN via epigenetic and/or microRNA-dependent control mechanisms. The epigenetic control of ISG expression and its impact on antiviral responses has been reported[17–20]. Accordingly, treatment of CN with an HDAC inhibitor reduced WNV yield and resulted in de-repression of expression of ISG at the basal level. One caveat to these studies is that inconsistent ISG expression phenotypes have been observed with HDAC inhibitors[46,47], although these differences may reflect variation in cell types, or concentration and time of inhibitor incubation. Our experiments also revealed higher expression in CN compared to GCN of microRNA-132, which targets the p300 co-activator of Stat1; ectopic expression of microRNA-132 in GCN decreased basal expression of ISGs. Distinct antiviral programs observed between GCN and CN may be explained by differences in the epigenetic state of key genes, which is influenced by the expression of microRNA.

In summary, we provide compelling evidence that specific neurons from disparate regions of the brain are differentially permissive to viral replication due to intrinsically distinct host defense programs. Our study also identifies novel antiviral genes in the CNS that restrict infection by WNV and other CNS viruses. This analysis may be relevant for understanding regional infection and immune responses against other pathogens of the CNS.

METHODS

Mice

C57BL/6 wild-type and congenic *Ifnar*$^{-/-}$ mice were bred in the animal facility of Washington University School of Medicine, and experiments were performed according to the guidelines and with approval of the Washington University Animal Studies Committee.

Preparation of primary neurons

CN and GCN were prepared from wild type mice as described[48].

Virus stocks

The WNV-NY strain (New York 1999) was passaged once in C6/36 *Aedes albopictus* cells to generate an insect cell-derived stock, and one additional time in Vero cells to generate a mammalian cell-derived stock. The Madagascar-AnMg798 strain of WNV (WNV-MAD) was obtained from the World Reference Center of Emerging Viruses and Arboviruses and passaged in Vero cells. The generation and propagation of MHV (strain A59) has been described elsewhere[49]. SLEV (strain GHA-3) was a gift of A. Barrett (Galveston, TX) and was passaged in Vero cells. VEEV (strain TC-83) was a gift of I. Frolov (Birmingham, AL) and was passaged in Vero cells. Levels of virus in the supernatant from infected cells were titrated by focus-forming or plaque assays on BHK21-15, Vero, or L929 cells.

RNA preparation and microarray analysis

Three independent cultures of CN and GCN were left untreated (Mock) or treated with 100 IU/ml of mouse IFN-β (PBL Interferon Source) using a balanced design. Twenty-four hours following treatment, total RNA was isolated according to the manufacturer's protocol with an RNeasy kit (Qiagen) and microarray analysis was performed using Agilent RM 4×44 K microarrays using the manufacturer's one-color analysis protocol. Data were normalized with GeneData analyst 2.2.1. Differential gene expression between groups was determined by a 3-way ANOVA model. The Benjamini and Hochberg algorithm was used to control the false discovery rate (FDR) of multiple testing (FDR adjusted P value < 0.01; selected for genes showing more than 2-fold change; Partek Genomic Suite; Partek Incorporated). Heat maps for gene expression were created using Spotfire DecisionSite 9.1.1. Functional analysis of statistically significant gene expression changes was performed using Ingenuity Pathway Analysis (IPA; Ingenuity Systems).

qRT-PCR

cDNA was generated from RNA using random hexamers and Multiscribe reverse transcriptase (Applied Biosystems). Transcripts were quantified on a 7500 Fast Real-time

PCR system (Applied Biosystems) with Taqman primers and probe sets (Integrated DNA Technologies). Cellular levels of 18S ribosomal RNA were quantified in parallel by TaqMan analysis and used for normalization.

Lentivirus transduction and functional evaluation of ISGs

Lentiviral constructs encoding individual ISG were generated by PCR amplification from cDNA generated from GCN treated with IFN-β. ISGs were subcloned into FCIV vector[50] (generous gift from Y. Sasaki, St Louis, MO). Lentivirus particles were generated and three days post-transduction, neurons were infected at an MOI of 1 (WNV-NY and VEEV), or MOI of 0.1 (WNV-MAD, SLEV, and MHV). One day following infection, cells were stained for WNV antigen with an E protein-specific MAb (WNV E16[51]) by flow cytometry, and viral supernatants were harvested and titered by focus-forming or plaque assay.

shRNA gene silencing

Lentiviruses encoding shRNA targeting a gene of interest were obtained from the RNAi Core facility at Washington University School of Medicine. GCN were transduced with lentivirus particles as described above. shRNA knockdown efficiency was confirmed by qRT-PCR (data not shown). WNV replication in shRNA-transduced cells was evaluated as described above.

MicroRNA experiments

For microRNA detection, total RNA was harvested using a miRNeasy Kit (Qiagen) according to the manufacturer's protocol, reverse-transcribed using microRNA-specific primers, and quantitated by Taqman microRNA expression assay (Applied Biosystems). Sno202 levels were quantified in parallel by TaqMan analysis and used for normalization. For microRNA expression, lentiviruses expressing microR-132 or control microRNA were generated and used according to the manufacturer's protocol (Biosettia).

QuantiGene Plex 2.0 assay

Brain tissues were harvested from naïve mice, and differential RNA expression was quantitated by the QuantiGene Plex 2.0 assay (Affymetrix) according to the manufacturer's protocol. *Actb* and *Rpl19* genes were used for normalization of data.

Immunohistochemistry

Wild type mice were infected with 10^1 PFU of WNV via an i.c. route and euthanized at day 6 after infection. *Ifnar*$^{-/-}$ mice were infected with 10^1 PFU of WNV via an intracranial route, treated with humanized E16 MAb to prevent spread to visceral organs, and euthanized at day 4 after infection. Brains were harvested, cryoprotected/paraffin embedded, sectioned, and stained with rat antisera against WNV as described elsewhere[52]. Human brain sections were obtained from fatal WNV encephalitis cases (generously provided by B.K. Kleinschmidt-DeMasters (Denver, CO) and C.A. Wiley (Pittsburgh, PA)) and stained with rat antisera against WNV or non-immune sera as described above.

Statistical analysis

Parametric and non-parametric data were analyzed by a two-tailed Student's *t* test and Mann-Whitney test, respectively using Prism software (GraphPad Software). Microarray data were analyzed by ANOVA and the Benjamini and Hochberg algorithm was used to control the false discovery rate (FDR) of multiple testing (Partek Genomic Suite; Partek Incorporated).

Supplementary Material

Refer to Web version on PubMed Central for supplementary material.

Acknowledgments

We thank O. Koues and E. Oltz for the experimental discussions and suggestions, J. Patel and R. Klein for their contribution to the initial phase of the study, B. Bradel-Tretheway for help with initial study design and microarray analysis, Y. Sasaki for the lentiviral plasmids, H.W. Virgin for the *Stat1*$^{-/-}$ mice, and B.K. Kleinschmidt-DeMasters and C.A. Wiley for the human brain autopsy samples. NIH grants U54 AI081680 (Pacific Northwest Regional Center of Excellence for Biodefense and Emerging Infectious Diseases Research), U19 AI083019 (M.G. and M.S.D), and R01 AI074973 (M.G. and M.S.D.) supported this work. The funders had no role in study design, data collection and analysis, decision to publish, or preparation of the manuscript.

References

1. Ireland DDC, Stohlman SA, Hinton DR, Atkinson R, Bergmann CC. Type I interferons are essential in controlling neurotropic coronavirus infection irrespective of functional CD8 T cells. J Virol. 2008; 82:300–310. [PubMed: 17928334]
2. Schoneboom BA, Lee JS, Grieder FB. Early expression of IFN-alpha/beta and iNOS in the brains of Venezuelan equine encephalitis virus-infected mice. J Interferon Cytokine Res. 2000; 20:205–215. [PubMed: 10714557]
3. McGavern DB, Kang SS. Illuminating viral infections in the nervous system. Nat Rev Immunol. 2011; 11:318–329. [PubMed: 21508982]
4. Delhaye S, et al. Neurons produce type I interferon during viral encephalitis. Proc Natl Acad Sci USA. 2006; 103:7835–7840. [PubMed: 16682623]
5. Wang J, Campbell IL. Innate STAT1-dependent genomic response of neurons to the antiviral cytokine alpha interferon. J Virol. 2005; 79:8295–8302. [PubMed: 15956575]
6. Griffin DE. Immune responses to RNA-virus infections of the CNS. Nat Rev Immunol. 2003; 3:493–502. [PubMed: 12776209]
7. Chakraborty S, Nazmi A, Dutta K, Basu A. Neurons under viral attack: Victims or warriors? Neurochemistry International. 2010; 56:727–735. [PubMed: 20206655]
8. Omalu BI, Shakir AA, Wang G, Lipkin WI, Wiley CA. Fatal fulminant pan-meningo-polioencephalitis due to West Nile virus. Brain Pathol. 2003; 13:465–472. [PubMed: 14655752]
9. Gordon B, Selnes OA, Hart J Jr, Hanley DF, Whitley RJ. Long-term cognitive sequelae of acyclovir-treated herpes simplex encephalitis. Arch Neurol. 1990; 47:646–647. [PubMed: 2346392]
10. Samuel MA, Diamond MS. Alpha/beta interferon protects against lethal West Nile virus infection by restricting cellular tropism and enhancing neuronal survival. J Virol. 2005; 79:13350–13361. [PubMed: 16227257]
11. Lazear HM, Pinto AK, Vogt MR, Gale M Jr, Diamond MS. Beta interferon controls West Nile virus infection and pathogenesis in mice. J Virol. 2011; 85:7186–7194. [PubMed: 21543483]
12. Armah HB, et al. Systemic distribution of West Nile virus infection: postmortem immunohistochemical study of six cases. Brain Pathol. 2007; 17:354–362. [PubMed: 17610522]
13. Keller BC, et al. Resistance to alpha/beta interferon is a determinant of West Nile virus replication fitness and virulence. J Virol. 2006; 80:9424–9434. [PubMed: 16973548]

14. Perwitasari O, Cho H, Diamond MS, Gale M Jr. Inhibitor of κB kinase epsilon (IKK(epsilon)), STAT1, and IFIT2 proteins define novel innate immune effector pathway against West Nile virus infection. J Biol Chem. 2011; 286:44412–44423. [PubMed: 22065572]
15. Schoggins JW, et al. A diverse range of gene products are effectors of the type I interferon antiviral response. Nature. 2011; 472:481–485. [PubMed: 21478870]
16. Brien JD, et al. Interferon regulatory factor-1 (IRF-1) shapes both innate and CD8(+) T cell immune responses against West Nile virus infection. PLoS Pathog. 2011; 7:e1002230. [PubMed: 21909274]
17. Fang TC, et al. Histone H3 lysine 9 di-methylation as an epigenetic signature of the interferon response. J Exp Med. 2012; 209:661–669. [PubMed: 22412156]
18. Agalioti T, et al. Ordered recruitment of chromatin modifying and general transcription factors to the IFN-beta promoter. Cell. 2000; 103:667–678. [PubMed: 11106736]
19. Parekh BS, Maniatis T. Virus infection leads to localized hyperacetylation of histones H3 and H4 at the IFN-beta promoter. Mol Cell. 1999; 3:125–129. [PubMed: 10024886]
20. Shestakova E, Bandu MT, Doly J, Bonnefoy E. Inhibition of histone deacetylation induces constitutive derepression of the beta interferon promoter and confers antiviral activity. J Virol. 2001; 75:3444–3452. [PubMed: 11238870]
21. Horvai AE, et al. Nuclear integration of JAK/STAT and Ras/AP-1 signaling by CBP and p300. Proc Natl Acad Sci USA. 1997; 94:1074–1079. [PubMed: 9037008]
22. Bhattacharya S, et al. Cooperation of Stat2 and p300/CBP in signalling induced by interferon-alpha. Nature. 1996; 383:344–347. [PubMed: 8848048]
23. Look DC, et al. Direct suppression of Stat1 function during adenoviral infection. Immunity. 1998; 9:871–880. [PubMed: 9881977]
24. Vo N, et al. A cAMP-response element binding protein-induced microRNA regulates neuronal morphogenesis. Proc Natl Acad Sci USA. 2005; 102:16426–16431. [PubMed: 16260724]
25. Wayman GA, et al. An activity-regulated microRNA controls dendritic plasticity by down-regulating p250GAP. Proc Natl Acad Sci USA. 2008; 105:9093–9098. [PubMed: 18577589]
26. Lagos D, et al. miR-132 regulates antiviral innate immunity through suppression of the p300 transcriptional co-activator. Nat Cell Biol. 2010; 12:513–519. [PubMed: 20418869]
27. Olsen L, Klausen M, Helboe L, Nielsen FC, Werge T. MicroRNAs Show Mutually Exclusive Expression Patterns in the Brain of Adult Male Rats. PLoS ONE. 2009; 4:e7225. [PubMed: 19806225]
28. Kim J, et al. A MicroRNA Feedback Circuit in Midbrain Dopamine Neurons. Science. 2007; 317:1220–1224. [PubMed: 17761882]
29. Contestabile A. Cerebellar granule cells as a model to study mechanisms of neuronal apoptosis or survival in vivo and in vitro. Cerebellum. 2002; 1:41–55. [PubMed: 12879973]
30. Fine EJ, Ionita CC, Lohr L. The history of the development of the cerebellar examination. Semin Neurol. 2002; 22:375–384. [PubMed: 12539058]
31. Fitting S, et al. Regional heterogeneity and diversity in cytokine and chemokine production by astroglia: differential responses to HIV-1 Tat, gp120, and morphine revealed by multiplex analysis. J Proteome Res. 2010; 9:1795–1804. [PubMed: 20121167]
32. Labrada L, Liang XH, Zheng W, Johnston C, Levine B. Age-dependent resistance to lethal alphavirus encephalitis in mice: analysis of gene expression in the central nervous system and identification of a novel interferon-inducible protective gene, mouse ISG12. J Virol. 2002; 76:11688–11703. [PubMed: 12388728]
33. Itsui Y, et al. Expressional screening of interferon-stimulated genes for antiviral activity against hepatitis C virus replication. J Viral Hepat. 2006; 13:690–700. [PubMed: 16970601]
34. Degrandi D, Hoffmann R, Beuter-Gunia C, Pfeffer K. The proinflammatory cytokine-induced IRG1 protein associates with mitochondria. J Interferon Cytokine Res. 2009; 29:55–67. [PubMed: 19014335]
35. Tal MC, Iwasaki A. Mitoxosome: a mitochondrial platform for cross-talk between cellular stress and antiviral signaling. Immunol Rev. 2011; 243:215–234. [PubMed: 21884179]

36. Szretter KJ, et al. The interferon-inducible gene viperin restricts West Nile virus pathogenesis. J Virol. 2011; 85:11557–11566. [PubMed: 21880757]
37. Fitzgerald KA. The interferon inducible gene: Viperin. J Interferon Cytokine Res. 2011; 31:131–135. [PubMed: 21142818]
38. Fentress SJ, et al. Phosphorylation of immunity-related GTPases by a Toxoplasma gondii-secreted kinase promotes macrophage survival and virulence. Cell Host Microbe. 2010; 8:484–495. [PubMed: 21147463]
39. Steinfeldt T, et al. Phosphorylation of mouse immunity-related GTPase (IRG) resistance proteins is an evasion strategy for virulent Toxoplasma gondii. PLoS Biol. 2010; 8:e1000576. [PubMed: 21203588]
40. Dellacasa-Lindberg I, Hitziger N, Barragan A. Localized recrudescence of Toxoplasma infections in the central nervous system of immunocompromised mice assessed by in vivo bioluminescence imaging. Microbes Infect. 2007; 9:1291–1298. [PubMed: 17897859]
41. Strittmatter C, Lang W, Wiestler OD, Kleihues P. The changing pattern of human immunodeficiency virus-associated cerebral toxoplasmosis: a study of 46 postmortem cases. Acta Neuropathol. 1992; 83:475–481. [PubMed: 1621505]
42. Zhao Y, et al. Virulent Toxoplasma gondii evade immunity-related GTPase-mediated parasite vacuole disruption within primed macrophages. J Immunol. 2009; 182:3775–3781. [PubMed: 19265156]
43. Cheon H, Stark GR. Unphosphorylated STAT1 prolongs the expression of interferon-induced immune regulatory genes. Proc Natl Acad Sci USA. 2009; 106:9373–9378. [PubMed: 19478064]
44. Hu X, Chakravarty SD, Ivashkiv LB. Regulation of interferon and Toll-like receptor signaling during macrophage activation by opposing feedforward and feedback inhibition mechanisms. Immunol Rev. 2008; 226:41–56. [PubMed: 19161415]
45. Amit I, et al. Unbiased reconstruction of a mammalian transcriptional network mediating pathogen responses. Science. 2009; 326:257–263. [PubMed: 19729616]
46. Nusinzon I, Horvath CM. Positive and Negative Regulation of the Innate Antiviral Response and Beta Interferon Gene Expression by Deacetylation. Mol Cell Biol. 2006; 26:3106–3113. [PubMed: 16581785]
47. Zupkovitz G, et al. Negative and Positive Regulation of Gene Expression by Mouse Histone Deacetylase 1. Mol Cell Biol. 2006; 26:7913–7928. [PubMed: 16940178]
48. Klein RS, et al. Neuronal CXCL10 directs CD8+ T-cell recruitment and control of West Nile virus encephalitis. J Virol. 2005; 79:11457–11466. [PubMed: 16103196]
49. Coley SE, et al. Recombinant mouse hepatitis virus strain A59 from cloned, full-length cDNA replicates to high titers in vitro and is fully pathogenic in vivo. J Virol. 2005; 79:3097–3106. [PubMed: 15709029]
50. Araki T, Sasaki Y, Milbrandt J. Increased nuclear NAD biosynthesis and SIRT1 activation prevent axonal degeneration. Science. 2004; 305:1010–1013. [PubMed: 15310905]
51. Oliphant T, et al. Development of a humanized monoclonal antibody with therapeutic potential against West Nile virus. Nat Med. 2005; 11:522–530. [PubMed: 15852016]
52. Shrestha B, Gottlieb D, Diamond MS. Infection and injury of neurons by West Nile encephalitis virus. J Virol. 2003; 77:13203–13213. [PubMed: 14645577]

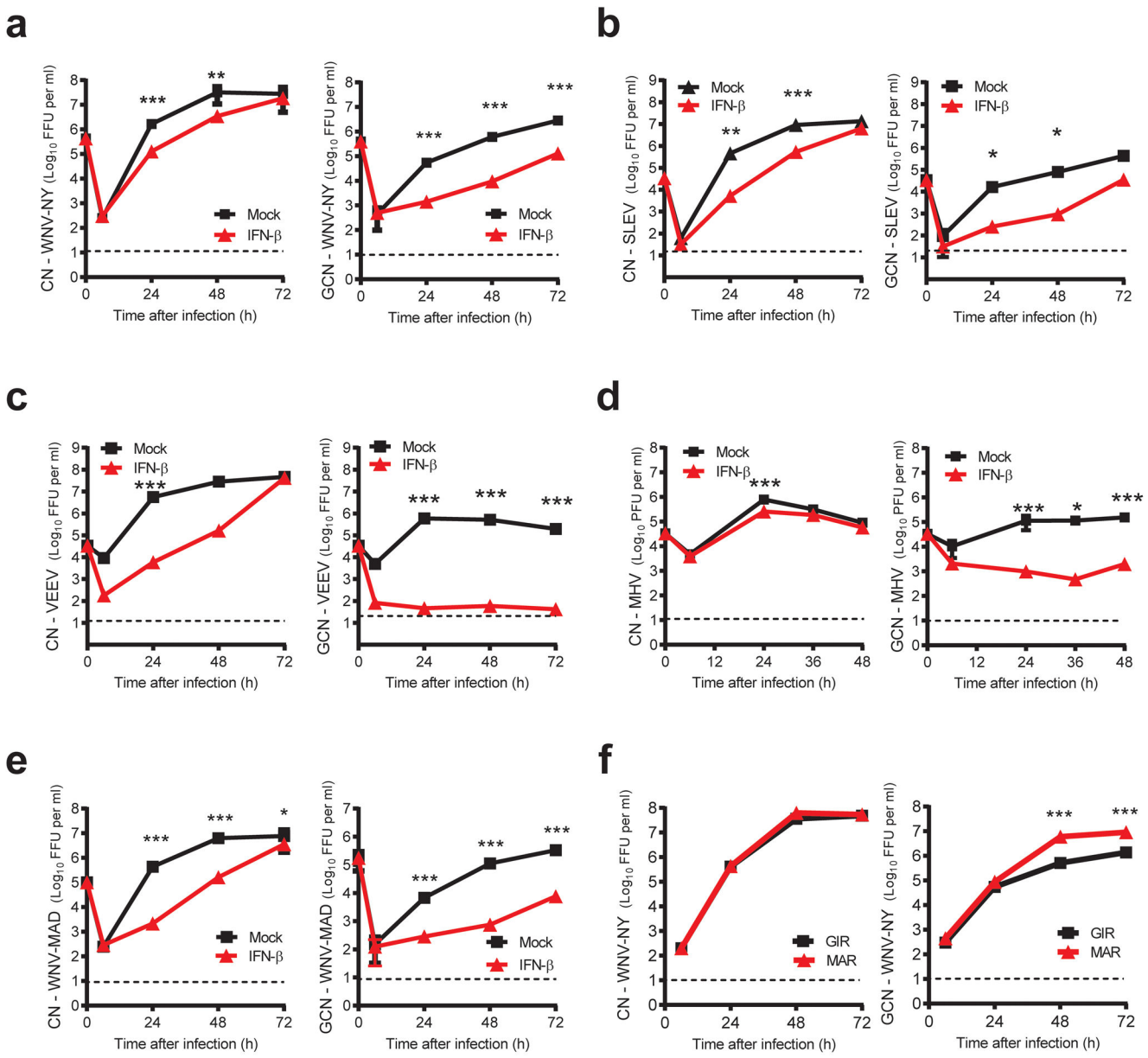

Figure 1. GCN are less susceptible to virus infection and more sensitive to the antiviral effects of IFN-β than CN

Infection of (**a**) WNV-NY, (**b**) SLEV, (**c**) VEEV, (**d**) MHV, and (**e**) WNV-MAD in primary neurons. Primary CN and GCN generated from wild-type mice were pre-treated with medium (Mock) or IFN-β (100 IU/ml), infected at an MOI of 0.1 (WNV-NY and WNV-MAD) or 0.01 (VEEV, SLEV, and MHV), and virus production was evaluated at the indicated time points. (**f**) GCN and CN were treated with 20 μg/ml of MAR1-5A3 (MAR) anti-Ifnar MAb or an isotype control MAb (GIR-208 (GIR)) and viral replication was monitored. Results are the average of three independent experiments performed in triplicate and asterisks (*, $P < 0.05$; **, $P < 0.01$; ***, $P < 0.0001$) indicate differences that are

statistically significant by an unpaired *t* test. Error bars indicate standard deviations (SD), and dashed lines indicate the limit of sensitivity of the assay.

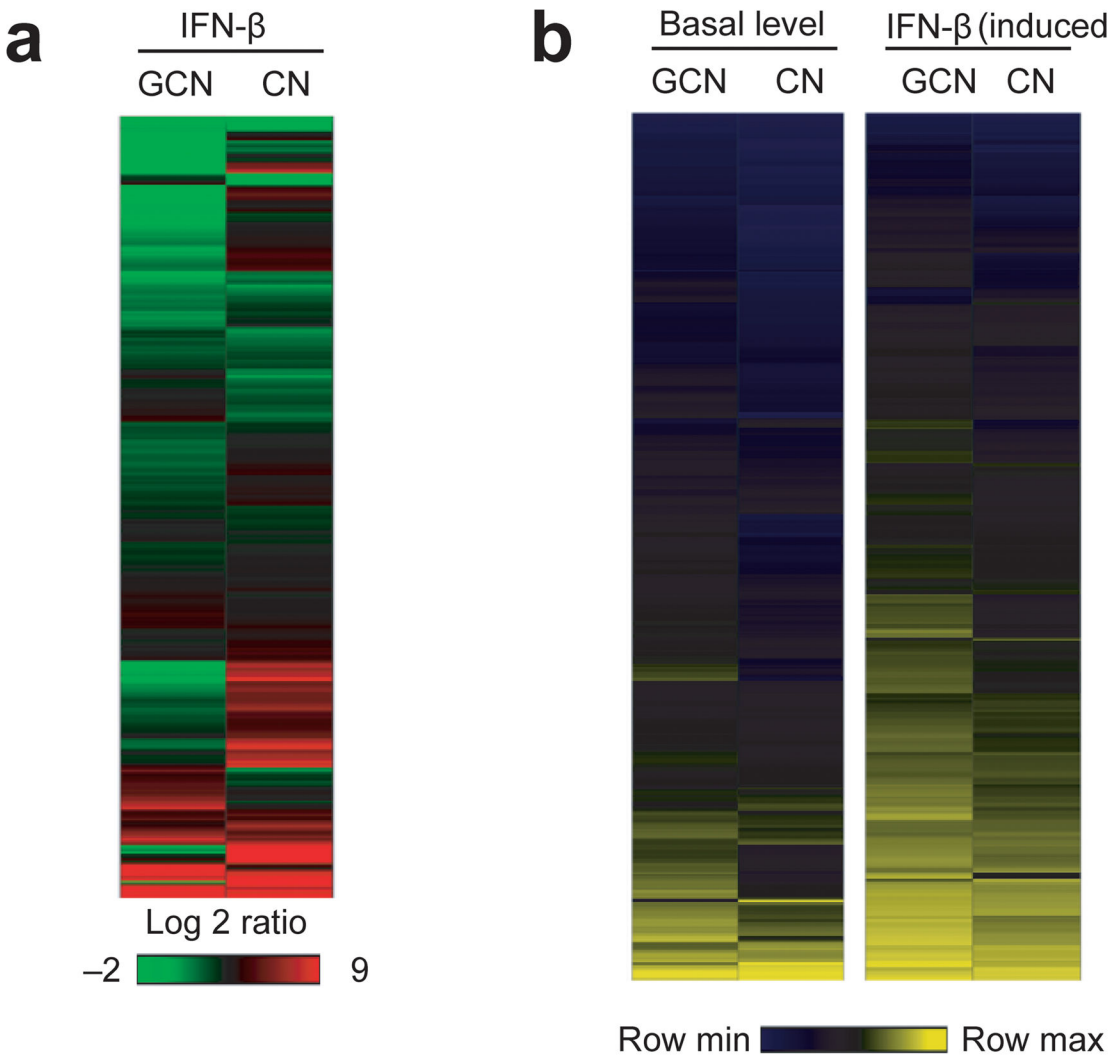

Figure 2. Microarray analysis reveals differential regulation of antiviral genes in GCN and CN

(**a**) Global view of gene expression 24 hours after IFN-β treatment (100 IU/ml). Clustering was performed using the hierarchical unweighted-pair group method using average linkages with a Euclidean distance similarity measure and average value ordering function. Data shown was compared to values from mock-treated cells (fold change). (**b**) Differential gene expression profile of IFN-β responsive genes identified by ANOVA approach (within cutoff values of a ≥ 2-fold change, Benjamini-Hochberg-adjusted *P* value of < 0.01). Shown are heat maps reflecting expression of IFN-β responsive genes (rows) at the basal level (left columns) or after IFN-β treatment (right columns) in GCN and CN.

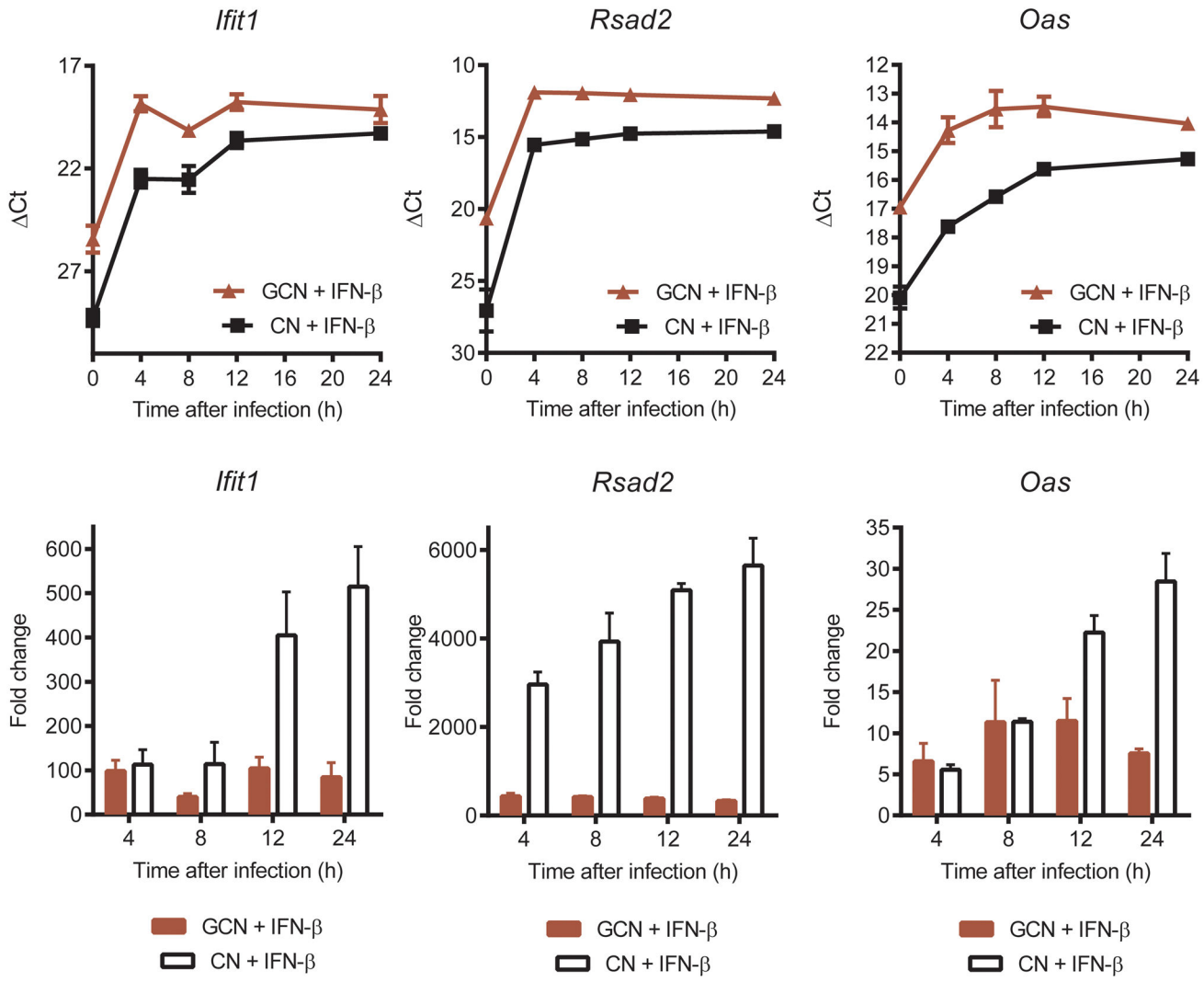

Figure 3. Key ISGs reach peak expression sooner and at higher levels in GCN

GCN and CN were treated with IFN-β (100 IU/mL) and cellular RNA was harvested at the indicated time points after treatment. Expression level and induction pattern of selected genes was evaluated by qRT-PCR. The results are the representative of three independent experiments performed in triplicate. The data is displayed as (*top*) the ΔCt value compared to cellular levels of 18S ribosomal RNA or (*bottom*) the fold change in expression compared to untreated cells.

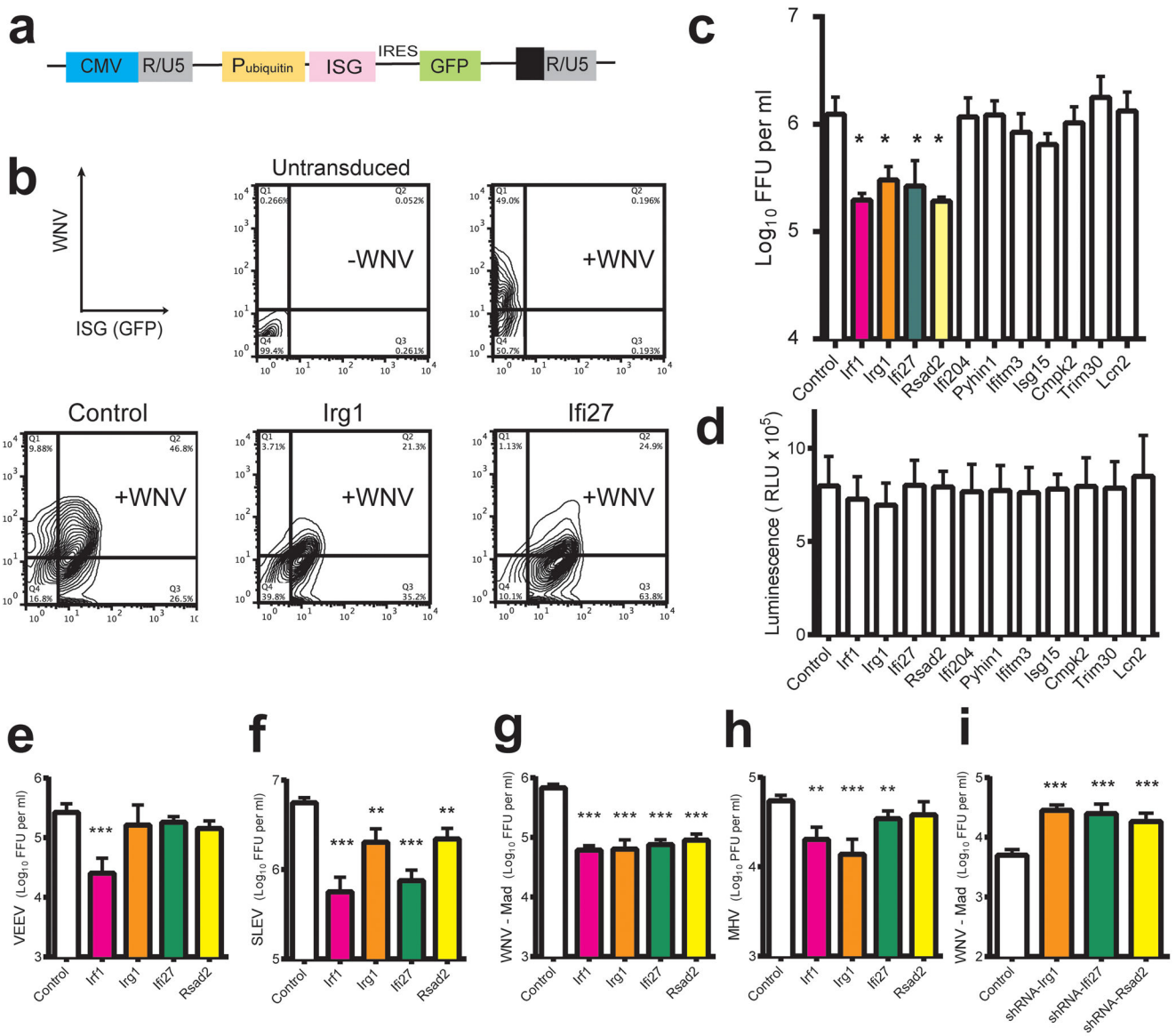

Figure 4. ISGs with antiviral activity were identified in neurons using a lentivirus transduction system

(**a**) Design of the bicistronic lentiviral vector. CMV, immediate early promoter from human cytomegalovirus; P-ubiquitin, ubiquitin promoter; IRES, internal ribosome entry site; and R/U5, HIV-1 long-terminal repeat. (**b**) Flow cytometry contour plots showing *Irg1* and *Ifi27*-mediated inhibition of WNV in primary cortical neurons. *x* and *y* axes indicate transduction efficiency (GFP intensity) and infectivity (level of WNV antigen), respectively. A packaged empty lentiviral vector was used as the negative control. (**c**) Results of focus-forming assays showing inhibition of WNV replication in CN transduced with *Irf1*, *Irg1*, *Ifi27*, and *Rsad2* but not with several other candidate genes (e.g., *Ifi204*, *Pyhin1*, *Ifitm3*, *Isg15*, *Cmpk2*, *Trim30*, and *Lcn2*). (**d**) After lentivirus transduction, cell viability was determined using a Cell-titer Glo luminescence-based assay. (**e–h**) Antiviral effects of *Irf1*, *Irg1*, *Ifi27*, and *Rsad2* in CN against (**e**) VEEV, (**f**) SLEV, (**g**) WNV-MAD, and (**h**) MHV.

(i) Lentiviruses expressing shRNA targeting *Irg1*, *Ifi27*, and *Rsad2* were transduced in GCN and viral replication was evaluated by focus-forming assay. shRNA targeting GFP was used as a control. For panels **c–i**, results are the average of at least three independent experiments, and asterisks (*, $P < 0.05$; **, $P < 0.01$; ***, $P < 0.0001$) indicate differences that are statistically significant by an unpaired *t* test. Error bars indicate SD.

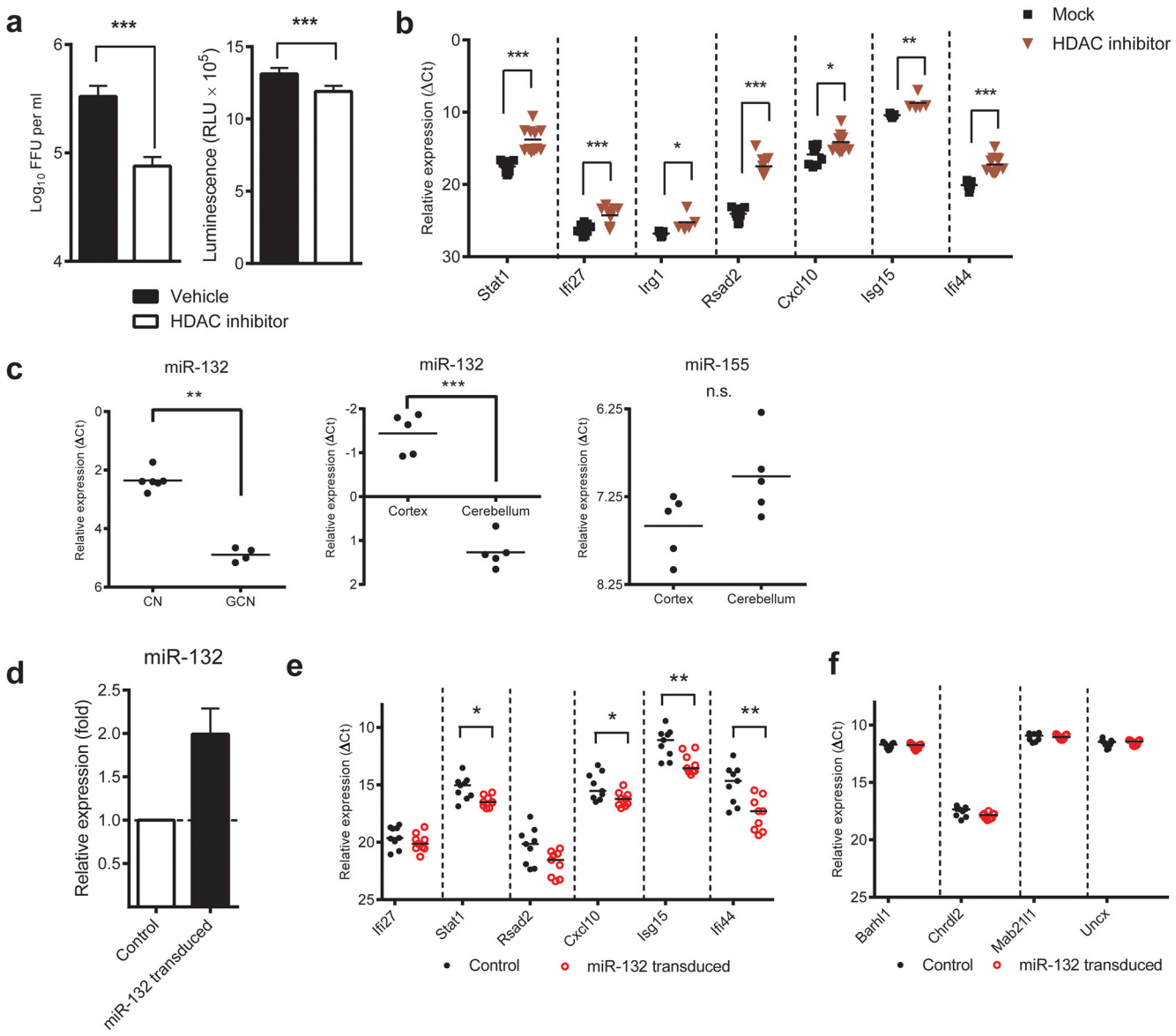

Figure 5. Epigenetic and microRNA-mediated control mechanism of ISGs

(**a**) CN were pre-treated with HDAC inhibitor, trichostatin A (TSA, 500 nM) or vehicle (0.1% (v/v) DMSO) for 12 hours, infected with WNV (MOI of 1), and virus production in the supernatant 12 hours later was evaluated by focus-forming assay. Results are the average of three experiments performed in triplicate. Error bars indicate SD (***, $P < 0.0001$) (*left)*. Twenty-four hours after TSA treatment, cell viability was determined using a Cell-titer Glo luminescence-based assay (*right)*. (**b**) CN were treated with TSA and expression level of the indicated genes was evaluated by qRT-PCR. The results are the average of three independent experiments performed at least in duplicate. The data is displayed as the ΔCt value compared to cellular levels of 18S ribosomal RNA. Solid lines represent the median values and asterisks indicate statistically significant differences (*, $P < 0.05$; **, $P < 0.01$; ***, $P < 0.0001$). (**c**) microRNA-132 (miR-132) expression levels in total RNA isolated

from GCN and CN were quantitated by qRT-PCR. The result is representative of four independent experiments with technical replicates of n = 2 to 6 per experiment. miR-132 and miR-155 (as a control) expression levels in total RNA isolated from cerebellum and cerebral cortex from five naïve C57BL/6 mice were quantitated by qRT-PCR. The data is displayed as the ΔCt value compared to cellular levels of sno202, a small RNA that is used commonly for microRNA normalization. Solid lines indicate median values. (**d**) miR-132, (**e**) ISGs, and (**f**) non-ISGs expression levels from total RNA isolated from GCN transduced with miR-132-expressing lentivirus were quantitated by qRT-PCR. The miR-132 level was normalized to the cellular level of sno202. Levels of ISGs were normalized to cellular level of 18S ribosomal RNA. Solid lines indicate standard deviations (miR-132) or median value (non-ISGs and ISGs). Asterisks indicate statistically significant differences (*, $P < 0.05$ **, $P < 0.001$; ***, $P < 0.0001$) as judged by the Mann-Whitney test.

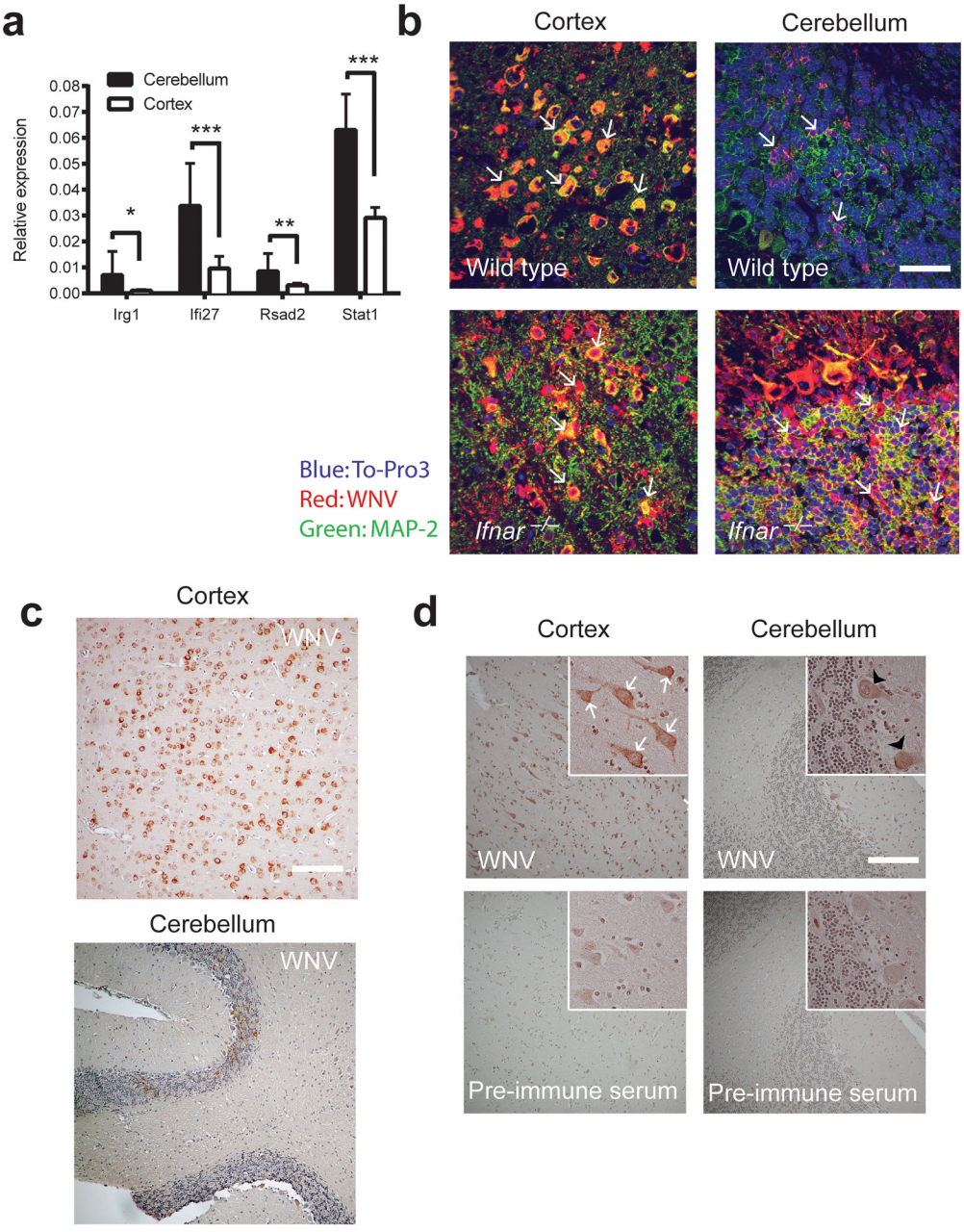

Figure 6. Differential WNV infection of neurons in the brains of mice and humans

(**a**) Differential gene expression of *Ifi27*, *Irg1*, *Rsad2*, and *Stat1* in the cerebellum and cortex of naïve wild-type mice as quantitated by QuantiGene Plex branched DNA amplification assay. The data was generated from eight mice, and the analysis was performed with triplicate samples for each mouse. Error bars indicate SD and asterisks indicate statistically significant differences (*, $P < 0.05$ **, $P < 0.001$; ***, $P < 0.0001$). (**b**) Brains from wild type and *Ifnar*$^{-/-}$ C57BL/6 mice were harvested at day 6 after i.c. infection with 10^1 PFU of WNV, cryoprotected, sectioned, and stained with rat anti-WNV antisera (red), an antibody to the neuronal marker MAP-2 (green), and ToPro-3 (blue) for nuclear staining. Representative images from the cerebellum and cerebral cortex are shown from five mice.

White arrows denote infected cells. Scale bar, 20 μm. (**c**) Brains from wild type C57BL/6 mice were harvested at day 6 after i.c. infection with 10^1 PFU of WNV, paraffin-embedded, sectioned, and stained with rat anti-WNV antisera (viral antigen, *brown*) and haematoxylin for nuclear staining (*blue*). Scale bar, 80 μm. (**d**) Brain sections of the cerebral cortex and cerebellum from a fatal human case of WNV encephalitis after staining with rat anti-WNV antisera (viral antigen, *brown*) or pre-immune sera. Infected CN and Purkinje neurons are indicated by white arrows and black arrow heads, respectively. Scale bar, 80 μm.